

# Low-cost photogrammetry solutions for surveying confined underground spaces: testing the traditional set-up against 360° camera on Tombs of the Kings archaeological site

Dimitrios Skarlatos<sup>1\*</sup>, Branka Cuca<sup>2</sup>, Georgios Kafataris<sup>1</sup>, Mattia Previtali<sup>2</sup>, Athos Agapiou<sup>1</sup>

<sup>1</sup> CUT, Cyprus University of Technology, Cyprus – dimitrios.skarlatos; gil.kafataris; athos.agapiou@cut.ac.cy

<sup>2</sup> POLIMI, Politecnico di Milano, Italy – mattia.previtali; branka.cuca@polimi.it

## Commission II

**Keywords:** low-cost photogrammetry, underground tomb chambers, 3D reconstruction, 360 camera, UNESCO WHS

## Abstract

This study explores low-cost photogrammetry solutions for surveying confined underground spaces, focusing on Tomb 7 at the UNESCO World Heritage Site, Tombs of the Kings in Paphos, Cyprus. The research, part of the ENGINEER project, compares traditional photogrammetric methods using frame cameras against a 360° multi-lens camera. The aim is to identify reliable, low-cost methods for 3D documentation of archaeological sites, which can be used for structural analysis and systematic monitoring. Three photogrammetric acquisition methodologies were tested: handheld with frame camera, standard with frame camera, and relaxed with 360° camera. The study evaluates the accuracy of these acquisition methods by comparing dense point clouds generated from each dataset against a reference dataset obtained via terrestrial laser scanning (TLS). Metrics such as cloud-to-cloud distance, roughness, and point cloud density were used for comparison. Results indicate that while the 360° camera offers ease of use and high data density, it also introduces more noise and variability. Traditional methods, though more time-consuming, provide more consistent and accurate results. The findings suggest that combining both approaches could optimize data quality and acquisition efficiency, making the 360° multi-lens camera a viable low-cost photogrammetry option for heritage documentation.

## 1. Introduction

Photogrammetry for cultural heritage documentation has always been a captivated subject, especially for its potential for replicability even with low-cost (and/or reasonable cost) equipment. In this paper we describe an exercise conducted within a wider framework of the ENGINEER project. The aim of this project is to enhance the collaboration between the experts from the fields of geomatics and civil engineering, and to adopt best practices related to the documentation of archaeological and cultural heritage sites or monuments in Cyprus, focusing on 3D-modelling for structural analysis. From the perspective of geomatics and geometric recording, the ultimate purpose of this kind of documentation would be to ensure an easy-to-implement and easy-to-replicate procedures that could foster a more systematic monitoring of monuments and sites over time. On the other side, with the results proposed here, colleagues dealing with structural analysis could rely on the re-use of a multitude of models and texture information to observe, measure and monitor possible changes over time in the structure, in material loss, modifications of cracking patterns and so forth.

### 1.1 Case study: UNESCO World Heritage Site Tombs of the Kings in Paphos, Cyprus

This paper tries to address some challenges when surveying confined underground and narrow spaces such as tombs, caves or narrow corridors, including lighting conditions, lack of space for the instruments, lack of professional illumination, limited acquisition time, etc.

The work presented in this paper was conducted in Paphos District in western Cyprus, in an UNESCO World Heritage Site (WHS): the town of Kato Paphos, in particular the necropolis known as Tafoi ton Vasileon (“Tombs of the Kings”). The specific case study illustrated is Tomb 7 (Figure 1) of the complex. Surveying activities presented here are part of a wider

heritage recording, documentation and monitoring process conducted in the framework of project ENGINEER coordinated by the Cyprus University of Technology (Agapiou et al., 2023).



Figure 1. Tomb 7, 3D textured mesh from oblique drone photos. Arrow shows the south-east wall used for comparison.

### 2. Examples of heritage recording techniques, including low-cost image acquisition, for advanced surface modelling

Difficulties such as manoeuvrability, sparse illumination, acquisition range, execution time, and error propagation are often found as a challenge during surveying and dense mapping of narrow spaces such as corridors, tunnels, caves and tombs. Often, laser scanning and photogrammetric techniques are employed contemporarily, while in some cases one is chosen over the other for reasons linked to size and accessibility of spaces, availability, or for purposes of comparing the performance of different technologies in challenging conditions.

In addition to topographic techniques necessary for landscape description, Banfi et al. (2023) employ terrestrial laser scanning

(TLS) and extensive photogrammetric survey to provide a full digital twin, and successively an extended reality environment, of the Neanderthal man and Lamalunga cave in Italy. This well preserved but highly fragile case study required high level of attention during the survey planning phase; different types of photogrammetric sensors were required to provide different resolution models according to the object of survey, ranging from complex cave surface to animal and human remains of extreme fragility. Authors argued the need for an integrated surveying approach in order to implement a method capable of transforming initial point clouds and mesh models into sophisticated virtual environments of these precious yet inaccessible archaeological remains.

Another example is provided by Biolo et al. (2023) as they employ laser scanner and photogrammetry techniques to survey the Torre della Colubrina the Porta del Soccorso, in proximity of the Castello Sforzesco in Milan. Narrow corridors that lead to these underground spaces have also been recorded with an extensive survey campaign in an attempt to successively propose a 3D model reconstruction that would allow to possibly define a correct location of the underground features in respect the remains visible above the ground.

Recently, the use of a fisheye multi-camera system, capable of completing the three-dimensional digitization of complex and narrow spaces together with a high-resolution photographic documentation acquisition was explored by Perfetti et al. (2024). The method was applied on Castagneta Tower San Vigilio Castle (Bergamo, Italy), chosen to test techniques and processing strategies in very challenging conditions such as long spaces with reduced transversal dimensions and lack of light.

Some previous studies have also compared accuracies between data generated from laser scanner and photogrammetric techniques. In Masiero et.al (2018), for example, at the medieval bastion in Padua authors explore the performances of the state-of-art portable laser scanner system (Leica Pegasus system) and a low-cost/high-portability system based on the use of photogrammetry and ultra-wide band (UWB) sensors. For both systems, the comparison was performed with the 3D model obtained from a TLS survey.

In this framework, and given the extensive geometric recording conducted for Tombs of the Kings site, it appeared suitable to propose a confrontation exercise between different datasets acquired using low-cost solutions. The overall objective of the comparison is to provide suggestion for a reliable and low-cost method for surveys in indoor and narrow spaces such as tombs, which would possibly require low acquisition expertise and minimal human effort. If identified, such method can be relatively easily replicated for a systematic recording and 3D model reconstruction of endangered archaeological structures, such as the case of Tomb 7 and other tombs of this complex.

### 3. Methodology

The comparison focuses on the accuracy evaluation of three photogrammetric acquisition methodologies. The three acquisition methodologies used differ both in camera used and acquisition approach: free handheld using frame camera, strict photogrammetric using frame camera, 360° multi lens camera in almost arbitrary positions (Fig., 3, 4, 5). The former one is based on an empirical approach for photograph acquisition, heavily relying on experience to ensure overlaps. This is a flexible approach where the operator adjusts the angles and positions of the camera to reduce acquisition time, adjust to object's geometry for coverage maximization, while maintaining adequate overlaps

for Structure from Motion (SfM). The second one represents the standardized acquisition protocol with parallel camera axis and 80% overlap, slightly adjusted for the peculiarities of the Tomb. Among the three datasets, the use of the 360° camera has significant impact on the acquisition protocol. Since this technology has been recently introduced in the photogrammetric workflow and there is not sufficient literature to describe a standardized acquisition protocol, almost arbitrary positions were selected. The advantage of this method is that even inexperienced operators will be able to acquire a useful dataset, with enough overlaps to ensure processing using SfM.

Although the entirety of Tomb 7 was documented, using a combination of aerial and terrestrial photogrammetry, as well as terrestrial laser scanning (TLS), the area of comparison was limited to one wall of the atrium. The comparison was performed on the left wall as seen when entering from the narrow corridor (south-east wall). A large dominant crack was evident on this wall and the geometric documentation was focused on it for structural reasons.

Dataset	Reference	Dataset 1	Dataset 2	Dataset 3
Instrument	Faro Focus S70 TLS	Nikon D780, 20mm prime lens	Canon 550D, 18-55mm zoom lens	XPhase pro X2
Sensor resolution	1.5mm/10m	Full frame, 24.5 MP, 6µm pixel	APS-C, 18MP, 4µm pixel	25 x 8MP, 134MP stitched panorama, 1.4µm pixel
Real focal length [mm]		20	Variable 10-18	3.85
Number of scans/images for Tomb 7	29 scans	74	136	114
Number of images used for the wall	-	26	66	20
Survey period	June 2023	June 2023	June 2023	July 2024
Acquisition time for Tomb 7 [min]	240	23 (wall only)	240	133
Average time per photo [min]	-	0.9	1.8	1.2

Table 1. Details of the datasets and equipment used.



Figure 2. A screenshot of the Tomb 7 TLS co-registered point cloud: atrium and colonnade area (above) and details of the burial chamber (below).

The complete data sets (all photos of the atrium) were processed in Agisoft's Metashape using same parameters, to generate a dense point cloud. The final dense clouds were compared to TLS

point cloud. Metrics used for comparison are described in paragraph 4.1 Results.

Table 1 summarizes the main characteristics of each dataset and some main elements of the surveying practice. The laser scanner dataset is referred to as a “reference dataset”, the dataset 1 as “handheld”, the dataset 2 as the “standard practice”, and dataset 3 as “360°” in this paper.

The following paragraphs report a brief description of acquisition technique applied for the LS reference dataset and for each of the Test datasets.

### 3.1 Laser scanner data acquisition: description of reference dataset

In this work the laser scanner dataset is used as a reference for the photogrammetry datasets. Although one may argue that TLS accuracy is not enough to act as reference for photogrammetric data, in this work TLS data were used to determine precision across the three datasets, rather than as a reference in strict metrological terms. The complexity and the size of Tomb 7 required the acquisition of 29 scans for both the external porch and corridor as well as for the interior spaces. The instrument used was a Faro Focus 3D S70. The measurement noise of the instrument is lower than  $\pm 2.0$  mm while the measurement accuracy is about  $\pm 1.0$  mm. Scans were registered using a target-based approach with both black and white checkerboard target and sphere target (Figure 2).

Six checkerboard targets were measured with a total station and served as ground control points for the georeferencing of the scans. A larger number of checkerboard and sphere targets were used as additional scan-to-scan correspondence improving the whole robustness of the registration. The final scan positioning was estimated using least squares adjustment with an average precision of  $\pm 3.3$  mm. Following the law of error propagation, we may assume an accuracy of 4.5 mm.

### 3.2 Photogrammetry dataset 1

This dataset was acquired with a Nikon D780 camera and a prime 20mm lens, in handheld mode and arbitrary positions, to cover the atrium, with emphasis on the wall under investigation; from now on. The aim was to acquire photos fast, ensuring maximum coverage for documenting the wall’s geometric complexity, ensuring enough overlaps for SfM processing, and adaptability on object’s geometry. The 20mm prime f/1.8G lens provided a large coverage, hence large overlaps for SfM processing were easily maintained. Figure 3 shows the images block geometry. It must be mentioned that this acquisition approach, although very fast (twice as fast as the standard approach, Table 1), heavily depends on the experience of the operator. In addition, replicability cannot be ensured when the same operator revisits the site to replicate the process for monitoring reasons.

Out of the 74 photos of the atrium, 26 were manually selected as the most appropriate to create the dense point cloud.



Figure 3. Images block geometry - Nikon D780.

### 3.3 Photogrammetry dataset 2

This dataset was collected using two self-calibrated zoom lenses (10-18mm and 18-135mm) The set-up was based on a “traditional” fixed-base and inline image acquisition with 80% overlap. The complete set was planned in four batches that correspond to the four walls of the atrium of Tomb7. Specific attention and additional images were taken at the connecting areas i.e. the angles of the atrium and the columns. Some difficulties there were identified during the dataset collection are the following:

1. This kind of technique is envisaged to provide very robust alignment but can result very time-consuming. However, for this specific case study a laser scanner survey and a drone photogrammetric survey were conducted in parallel, hence the coverage of the whole tomb was ensured. Based on this, photogrammetric coverage was focused on vertical surfaces and columns while the upper part of the tomb was omitted.
2. The corridor of the Tomb 7 leading to the atrium is a very narrow space (~1.5m width). A dataset of 80% of coverage would have requested an extremely short base (and hence a very high number of imagery), making both data acquisition and processing more challenging that would prolong the data acquisition time.
3. Image acquisition of the inside spaces was quite challenging due to their lighting conditions. Although the tripod and high exposition time was used, the images of these spaces still appeared with a dubious quality. The burial chambers of the Tomb (and especially the single graves) would probably require specific lighting step-up to respect the resolution and level of sharpness of the overall dataset.

Given the restrictions, the use of a frame camera in free hand mode, or the use of a 360 camera, could help in relaxing acquisition issues.

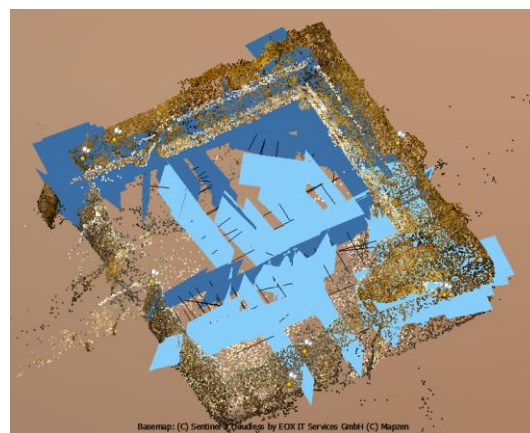


Figure 4. Images block geometry - Canon 550D.

### 3.4 Photogrammetry dataset 3

A low cost 360° camera (~1000€) was used for the acquisition. The camera houses in a rigid body, 25 cameras, 8Mp each, with normal lens. By default, it works in HDR mode with three or six bracketing photos. This is very useful when 360° cameras are utilized in places with strong bright and dark parts within the panorama image, such as in this example. On the other hand, the use of tripod is a necessity. The result is a stitched 134Mp panorama image, while the user has access to the raw bracketed photos of all cameras, 8MP each, should he wish to download them.

Since the camera by default ensures ample coverage with neighboring images, there is no need for precautions data acquisition. The operator needs to focus only on the distance



from object and following the geometry of the object, reducing its task load. This makes photogrammetric data capture a relatively easy task even for beginners, not familiar with photogrammetric protocols for data collection. Acquisition time (Table 1) is not significantly faster than the standard practice, because of the time needed to store the data volume of the bracketed photos and the time needed for the operator to remove himself from the camera's field of view. The relaxed image acquisition process and the large amount of data collected, make this approach interesting for further investigation (Pérez-García, J.L., et al., 2024).

Unfortunately, the 360° camera was not available during the initial field period (June 2023) and the images were acquired a year later. Hence, there were no targets nor ground control points available during the acquisition. Instead, the 360° images were processed with the Nikon D780 photos in a combined dataset to co-register all data. Results on Table 2 reflect the combined block processing. After the bundle adjustment, Nikon photos and several 360° images were removed, to generate the final point cloud only from 20 selected 360° images in the atrium. This demonstrates that the 360° may ease acquisition, by reducing the need for photos. This is enhanced when considering that these photos would be enough for the 3D reconstruction of the whole atrium. Nevertheless, when used in open space, most of the panorama image is occupied by the sky, reducing the effectiveness of the 360° camera.



Figure 5. 360 images block geometry - XPhase Pro X2.

### 3.5 Processing data sets

All processing was done in Agisoft's Metashape. For alignment 2.2K key points per Mpx and 4K tie points with guided matcing was selected, to ensure uniform density of points irrespectively of the camera resolution. Camera self-calibration was performed for  $f$ ,  $c_x$ ,  $c_y$ ,  $k_1$ - $k_3$ ,  $p_1$ ,  $p_2$ . Alignment was performed in high accuracy, ensuring high quality matching points between images. The dense cloud was created using High quality and Mild filtering. No filtering for gross errors was performed in alignment (bundle adjustment) phase nor in the generated point clouds. The three dense point clouds were clipped to the exact same area as the reference dataset, for comparison purposes. The basic parameters of the processing are reported in Table 2.

Both frame cameras demonstrated almost similar results, while 360° deviates in several aspects. There is significant difference in reprojection error among frame and 360° camera. The recorded information (total Mp in Table 2) and average GSD is in favour of the 360° camera, but the total tie points and reprojection error are worst than the frame cameras. This is the result of poor individual camera quality, poor camera calibration due to inconsistent stitching, and the fact that area of the panoramas is occupied by the sky, without any valuable information.

Dataset	Dataset 1	Dataset 2	Dataset 3
Number of photos	26	66	20
Total Mp	624	1188	2600
Average distance to object [m]	4.5	4	1.5
Average GSD [mm]	2	2	1
Tie points in 3D [K]	67	99	55
Average tie point multiplicity	3.5	4.5	3.7
Reprojection error [pixels]	0.66	1.00	2.27
Number of GCPs	6	7	6
Control point RMS (3D Total) [m]	0.005	0.006	0.005
Control points reprojection error [pixels]	0.35	1.2	0.5
Final clipped PC [Mpoints]	8.2	29.9	40.7

Table 2. Processing parameters and results for the different photogrammetric blocks / datasets.

Both frame cameras maintained a similar distance from the object, but the 360° was able to move closer to the object in an attempt to gather more details. This is also demonstrated by the fact that the average GSD for frame cameras being twice as the 360° one.

## 4. Discussion of the results

### 4.1 Results

The comparison among point clouds obtained from the different datasets was carried out in CloudCompare (<https://www.danielgm.net/cc/>) for the south-east facade of the tomb by using specific metrics to evaluate their characteristics and differences. The main parameters used for this comparison were:

**Unsigned Cloud-to-Cloud Distance:** This metric quantifies the distance between corresponding points in different point clouds without considering direction, providing an overall measure of similarity or variation between the clouds. Mean, value standard deviation and RMS (Root Mean Square) of discrepancies were evaluated.

**Roughness:** Roughness measures the variability in the surface geometry of the point cloud, reflecting surface texture and irregularities. This parameter helps assess differences in surface details between the point clouds as well as identifying noise in the outcomes. In this comparison two different radiuses were used for roughness computation (1.0 and 2.5 cm).

**Point Cloud Density:** Density reflects the concentration of points within a given area of the point cloud, offering insight into the level of detail and resolution of the data. By comparing point cloud densities, we could evaluate the coverage and granularity across different datasets. For the computation of surface density, a radius of 2.5 cm was used in this example.

These parameters enabled a detailed comparative analysis of the point clouds, highlighting differences in spatial alignment, surface characteristics, and data resolution. The results of the comparison presented are reported in Table 3 and graphically in Figures 6-8. Point cloud metrics concerning unsigned cloud-to-cloud distance exhibits a very similar value of mean point discrepancy and standard deviation for Dataset 1 and 2. Dataset 3 presents similar results in terms of mean discrepancy with respect to the other two datasets but with a larger standard deviation indicating more variability in the data and possibly higher noise. This is also confirmed by the roughness values

computed for Dataset 3 showing a rougher and more irregular surface with respect to the one computed for the other two datasets. Conversely Dataset 3 presents higher surface density with respect to the other ones. This can be explained by the lower average distance to object and better GSD characterizing this dataset.

The RMS error of all datasets (6.0mm, 5.5mm and 8.0mm) is above the 4.5mm estimated accuracy of the TLS, but not worse enough for the TLS to serve as reference data in a metrological sense. Roughness (Table 3, Figure 7), is consistently better in Dataset 1, demonstrating that quality of sensor-lens combination contributes to better surface model.

On another note, the photogrammetric point clouds under comparison, were not filtered at all, to enhance discrepancies and problems of each dataset. In an actual project scenario, filtering would have been performed in tie points and in final dense point cloud, improving final 3D reconstruction.

Metrics	TLS data	Dataset 1	Dataset 2	Dataset 3
Final clipped point cloud [Mpoints]	72.6	8.2	29.9	40.7
Mean discrepancy [mm]	-	4.8	4.6	5.7
Discrepancy std. dev. [mm]	-	3.6	3.0	5.6
RMS [mm]	-	6.0	5.5	8.0
Roughness at 1.0 cm [mm]	1.1	0.5	0.7	1.1
Roughness at 2.5 cm [mm]	2.0	1.2	1.6	2.3
Surface Density at 2.5 cm [points/m <sup>2</sup> ]	1995K	70K	256K	347K

Table 3. Results of datasets comparison.

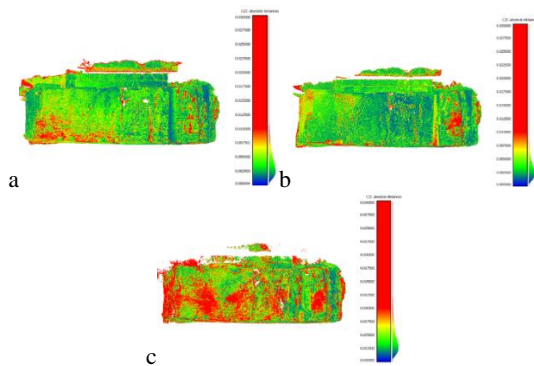


Figure 6. Unsigned Cloud-to-Cloud Distance comparison: a) Dataset 1, b) Dataset 2 and c) Dataset 3.

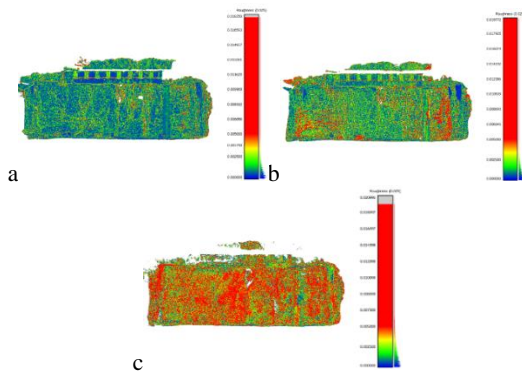


Figure 7. Roughness (2.5 cm) comparison: a) Dataset 1, b) Dataset 2 and c) Dataset 3.

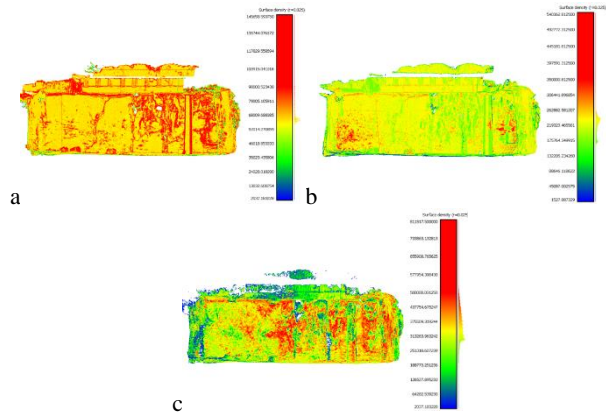


Figure 8. Surface Density (2.5 cm) comparison: a) Dataset 1, b) Dataset 2 and c) Dataset 3.

## 4.2 Discussion

Although Tomb 7 and surroundings were fully documented, including drone survey, this exercise focuses only on the south-east wall of the atrium (Figure 1), which is the wall with the larger visible crack and more complex geometry.

Different acquisition methods and equipment have been used to fully cover Tomb 7 internally and externally, in a complementary manner. There are large overlaps of data to ensure full coverage, redundancy and nourish future research activities such as this comparison. This comparison was not designed from scratch, but rather conceived in a later stage as a valid ENGINEER question, on ways to reduce acquisition time and cost. Therefore, our comparison is weak by academic definition. Nevertheless, addresses real world scenarios and questions on reducing equipment and acquisition cost while maintaining precision and accuracy standards for 3D reconstruction aiming in structural analysis and monitoring of CH monuments.

On the same note, results should be interpreted considering the quality and cost of the equipemnt. For example the reprojection error of the handheld method is lower than the the standard practise, but this might be attributed to the quality of the camera-lens combination (full frame with prime lens vs APS-C with zoom lens), rather than the acquisition method. The same statement holds for the low cost 360° which is significant cheaper (1/3 or less) to the full frame rig used for Dataset 1. Hence, the worst reprojection error and noisier point cloud are expected and verified by this comparison.

The use of handheld method doesn't seem to have significant advantage over the standard practice, other than the acquisition time. The quality difference on the results (Table 3) among the datasets 1 and 2, reflect the density of acquisition and quality of photos. The standard practice achieves a uniform quality, while the handheld is quicker but riskier. Combining both methods would achieve both uniform quality and increased detail and accuracy in specific areas, at the cost of increased acquisition time.

The 360° has demonstrated the larger reprojection error during bundle adjustment and the worse results during comparison. The final 3D reconstruction is denser due to high GSD and total Mpixels but it is noisier with RMS at least 33% worse than the frame cameras. This can be attributed to the uncontrolled stitching of the individual photos into a panorama, which cannot be effectively addressed by self-calibration during bundle adjustment. The 25 lens' distortions could only be effectively modelled if the camera is used as a fixed rig with 25 independent cameras.

The use of 360° in confined spaces is its major advantage, where all recorded data can be used both for alignment and 3D

reconstruction. On open spaces, sky coverage significantly reduces its value, while unnecessarily increases data storage and processing. The final 3D reconstruction is precise and accurate enough for the scope of structural analysis.

Other advantages of the use of the 360° camera include uniformity of data, the use of a single pipeline for all products, and the ability to create a textured 3D mesh model, which is invaluable for civil engineers when they try to identify and measure the width of cracks. Given that the final 3D reconstruction fulfills the accuracy standards of a given project in confined spaces, where the camera to object distance is small and in favor of the 360° camera, the specific equipment should be considered as a valid and low-cost alternative, with many benefits in terms of data acquisition effort.

The accuracy potential of the 360° camera as a rig of 25 independent cameras should be further investigated, as it proves invaluable equipment for photogrammetric projects in confined spaces.

### Acknowledgments

The authors would like to acknowledge the ENGINEER project. This project has received funding from the European Union's Horizon Europe Framework Programme (HORIZON-WIDERA2021-ACCESS-03, Twinning Call) under grant agreement No 101079377 and the UKRI under project number 10050486. Disclaimer: Views and opinions expressed are, however, those of the authors only and do not necessarily reflect those of the European Union or the UKRI. Neither the European Union nor the UKRI can be held responsible for them. The authors would also like to thank the Department of Antiquities of Cyprus for providing access to the site and for their support.

### References

Agapiou, A., Aktas, Y. D., Barazzetti, L., Costa, A., Cuca, B., D.' Ayala, D., Kyriakides, N., Kyriakidis, P., Lysandrou, V., Oreni, D., Previtali, M., Skarlatos, D., Tavares, A., Vlachos, M., 2023. Geomatics and civil engineering innovative research on heritage: introducing the "ENGINEER" project, *Int. Arch. Photogramm. Remote Sens. Spatial Inf. Sci.*, XLVIII-M-2-2023, 27–32. doi.org/10.5194/isprs-archives-XLVIII-M-2-2023-27-2023.

Banfi, F., Dellù, E., Stanga, C., Mandelli, A., Roncoroni, F., Sivilli, S., Pepe, G., and Cacudi, G., 2023. Representing intangible cultural heritage of humanity: from deep abyss of the past to Digital Twin and XR of the Neanderthal man and Lamalunga cave (Altamura, Apulia), *Int. Arch. Photogramm. Remote Sens. Spatial Inf. Sci.*, XLVIII-M-2-2023, 171–181. doi.org/10.5194/isprs-archives-XLVIII-M-2-2023-171-2023.

Biolo, F., Guzzetti, F., and Anyabolu, K. L. N., 2023. Integration of different types of survey output and the information asset in a 3D model of the Castello Sforzesco in Milan, *Int. Arch. Photogramm. Remote Sens. Spatial Inf. Sci.*, XLVIII-M-2-2023, 219–226. doi.org/10.5194/isprs-archives-XLVIII-M-2-2023-219-2023.

Masiero, A., Fissore, F., Guarnieri, A., Pirotti, F., Visintini, D., Vettore, A., 2018. Performance Evaluation of Two Indoor Mapping Systems: Low-Cost UWB-Aided Photogrammetry and Backpack Laser Scanning. *Applied Sciences*. 2018; 8(3):416. doi.org/10.3390/app8030416

Pérez-García, J.L., Gómez-López, J.M., Mozas-Calvache, A.T., Delgado-García, J., 2024. Analysis of the Photogrammetric Use of 360-Degree Cameras in Complex Heritage-Related Scenes: Case of the Necropolis of Qubbet el-Hawa (Aswan Egypt). *Sensors*. 2024, 24,2268. doi.org/10.3390/s24072268

Perfetti, L., Fassi, F., Vassena, G., 2024. Ant3D—A Fisheye Multi-Camera System to Survey Narrow Spaces. *Sensors*. 2024; 24(13):4177. doi.org/10.3390/s24134177

UNESCO World Heritage Center, 2024. Last accessed in July 2024 at <https://whc.unesco.org/en/list/79>